



Opinionated article

Giulia Guidetti, Yu Wang and Fiorenzo G. Omenetto*

Active optics with silk

Silk structural changes as enablers of active optical devices

<https://doi.org/10.1515/nanoph-2020-0358>

Received July 1, 2020; accepted July 16, 2020; published online August 1, 2020

Abstract: Optical devices have been traditionally fabricated using materials whose chemical and physical properties are finely tuned to perform a specific, single, and often static function, whereby devices' variability is achieved by design changes. Due to the integration of optical systems in multifunctional platforms, there is an increasing need for intrinsic dynamic behavior, such as devices built with materials whose optical response can be programmed to change by leveraging the material's variability. Here, regenerated silk fibroin is presented as an enabler of devices with active optical response due to the protein's intrinsic properties. Silk's abilities to controllably change conformation, reversibly swell and shrink, and degrade in a programmable way affect the form and the response of the optical structure in which it is molded. Representative silk-based devices whose behavior depends on the silk variability are presented and discussed with a particular focus on structures that display reconfigurable, reversibly tunable and physically transient optical responses. Finally, new research directions are envisioned for silk-based optical materials and devices.

Keywords: biomaterials; optics; reconfigurable; silk; transient; tunable.

Giulia Guidetti and Yu Wang: These authors contributed equally to this work.

***Corresponding author:** **Fiorenzo G. Omenetto**, Silklab, Department of Biomedical Engineering, Tufts University, Medford, MA 02155, USA; Laboratory for Living Devices, Tufts University, Medford, MA 02155, USA; Department of Physics, Tufts University, Medford, MA 02155, USA; and Department of Electrical and Computer Engineering, Tufts University, Medford, MA 02155, USA, E-mail: fiorenzo.omenetto@tufts.edu.
<https://orcid.org/0000-0002-0327-853X>

Giulia Guidetti and Yu Wang, Silklab, Department of Biomedical Engineering, Tufts University, Medford, MA 02155, USA; and Laboratory for Living Devices, Tufts University, Medford, MA 02155, USA. <https://orcid.org/0000-0002-6065-3359> (G. Guidetti). <https://orcid.org/0000-0003-0249-4414> (Y. Wang)

1 Introduction

Traditionally, optical devices have been fabricated so that their structure, material and, thus, designed function would either remain unchanged with time, being virtually immutable, or could undergo changes only due to external adaptations of their constructs. This design strategy ensures a practically constant performance as a function of time within the individual components' functional lifetime; additionally, it is based on materials whose properties have been highly engineered to fulfill one specific aim and are, optically, of very high quality [1]. This approach is very advantageous for the fabrication of optical devices that require high specialization and long durability; despite this, optical components built following this design strategy are strongly limited in multifunctionality and often lack inherent physical/chemical sensitivity and specificity to analytes, as they are programmed not to change.

The last few decades have seen a growing interest in materials with dynamic behaviors that are responsive to the environment that surrounds them. In particular, optical structures have been progressively integrated within electronic devices or biomedical platforms (to name a few), causing a shift in the materials and device design specifications. Specifically, new requirements emerged including the need for devices to be reconfigurable, tunable, and resorbable (and, therefore, temporally limited). In addition, the need for disposable devices requires materials with lower production costs and with minimal or no environmental hazards. To produce devices capable of such dynamic responses, it is necessary to change the optical device design strategy in terms of materials used and forms in which they are molded. The advantage of following this design strategy is in having devices which can be programmed to change their response as a function of a set of specific stimuli instead of having to fabricate a dedicated device for each of those stimuli. Regenerated silk protein features a combination of properties that makes it an ideal candidate to build such devices: among the many advantages offered by this biopolymer, the protein's abilities to controllably change conformation, reversibly swell and

shrink, and undergo a programmable degradation are key for integrating an active response in optical platforms.

Here, we present a critical overview of active optical devices that use regenerated silk fibroin as the stimuli-responsive component. We first provide a brief description of the regeneration of silk fibroin, of the manufacturing technologies that allow to transform aqueous silk solutions into multiple silk constructs, and of the silk's structural variability. Then, we discuss recent examples of active silk-based optical devices, focusing on reconfigurable, reversibly tunable, and physically transient optical systems. Finally, we comment on new research possibilities that can be enabled by silk's variable properties.

2 Silk for active optics

The ideal materials for active optical devices should demonstrate modulation across different scales. These range from modifications at the molecular level and at the nanoscale, such as variations in the refractive index and in the formed nanostructure, to macroscopic changes, such as swelling, strain ability, and solubility. These modifications affect the material's form and structural integrity, and, therefore, its overall optical response. Silk, as a naturally-derived biopolymer, can often satisfy those requirements due to its hierarchical structure, controllable transition between its polymorphic structures [2], reversible volume swelling and shrinking, and programmable biodegradability [3].

Silk can be extracted from the cocoons of the *Bombyx mori* lepidoptera, which are spun by the caterpillars during their metamorphosis [4–6]. Natural silk fibers are fabricated by dry spinning of a concentrated silk protein aqueous solution into an insoluble and hierarchically arranged bundle of silk fibroin microfibers surrounded by a sericin gluey layer [4,7]. Such insoluble silk fibers can be retransformed into aqueous solutions that can then be processed using multiscale fabrication technologies to give a variety of forms generating diverse optical responses. Silk cocoons are first degummed through a boiling process, then dissolved in a concentrated salt solution (usually LiBr) and, finally, transformed in an aqueous solution purified by dialysis [8] (Figure 1A). The resulting regenerated silk fibroin solution displays a combination of properties which converge into making silk fibroin an ideal building block for optical and photonic applications; these include nanoscale processability, water-based processing, ease of functionalization, and the capacity to form mechanically robust, highly optically transparent, thermally stable, and multifunctional materials.

Silk fibroin solutions can be processed using multiscale, water-based fabrication techniques to obtain a wide variety of multidimensional structures, including films, hydrogels, fibers, sponges, and solid blocks [10]. Remarkably, silk fibroin's relatively high thermal stability [11] and solubility in water allows it to be processed using a broad variety of already optimized multiscale fabrication techniques for optical and electronic devices without the need of dedicated fabrication processes [12]. Among the broad variety of biomanufacturing techniques available for silk processing, the ones mostly used for the fabrication of silk-based optical devices include electron beam lithography [13, 14], soft lithography [10, 15], photolithography [16], nanoimprinting [17, 18], inkjet printing [19, 20] direct ink writing [21], direct transfer [22], spin coating, and self-assembly [9, 20, 23]. Notably, as some of these techniques require energy transfer to the material being processed and can control its sol–gel–solid transition that can activate crosslinking [10, 13, 14, 17, 18], they can implicitly impart conformational changes to the protein, therefore modulating its water solubility during the fabrication of the material, without the need for post-treatments.

One of the key traits that distinguishes biopolymers from other materials is their variability. As a structural protein, silk fibroin undergoes conformational transition among β -sheets, random coils, and helices upon exposure to external stimuli, such as water vapor, methanol, and deep UV light (Figure 1B) [14, 24, 25]. The interactions between water/methanol molecules and the polar groups of silk fibroin chains can affect the hydrogen bonding between protein chains, thus leading to the conversion of a water-soluble material (amorphous silk) into a water-insoluble format (crystalline silk) by inducing the formation of β -sheets [24, 26]. By contrast, UV irradiation induces peptide chain scission and photodegradation of the silk fibroin initially at the weaker C–N bonds, giving rise to a considerable decrease in the protein's degree of crystallinity [27]. In practice, the higher the β -sheets content is, the higher the crystallinity and hence the lower the water solubility and the longer the functional lifetime of the silk structure. The final protein's conformation is crucial in determining both the silk material macroscopic physical properties and, especially, its modulation possibilities. The essence of silk's polymorphic transitions lies in the molecular rearrangement at the nanoscale, offering the possibility to create reconfigurable and programmable silk-based optical devices. At the same time, as a biodegradable material, the structural integrity of silk-based materials can be modulated when exposed to aqueous solutions or implanted *in vivo*. The dissolution and/or the biodegradation rates can be programmed to range from minutes to years by controlling the

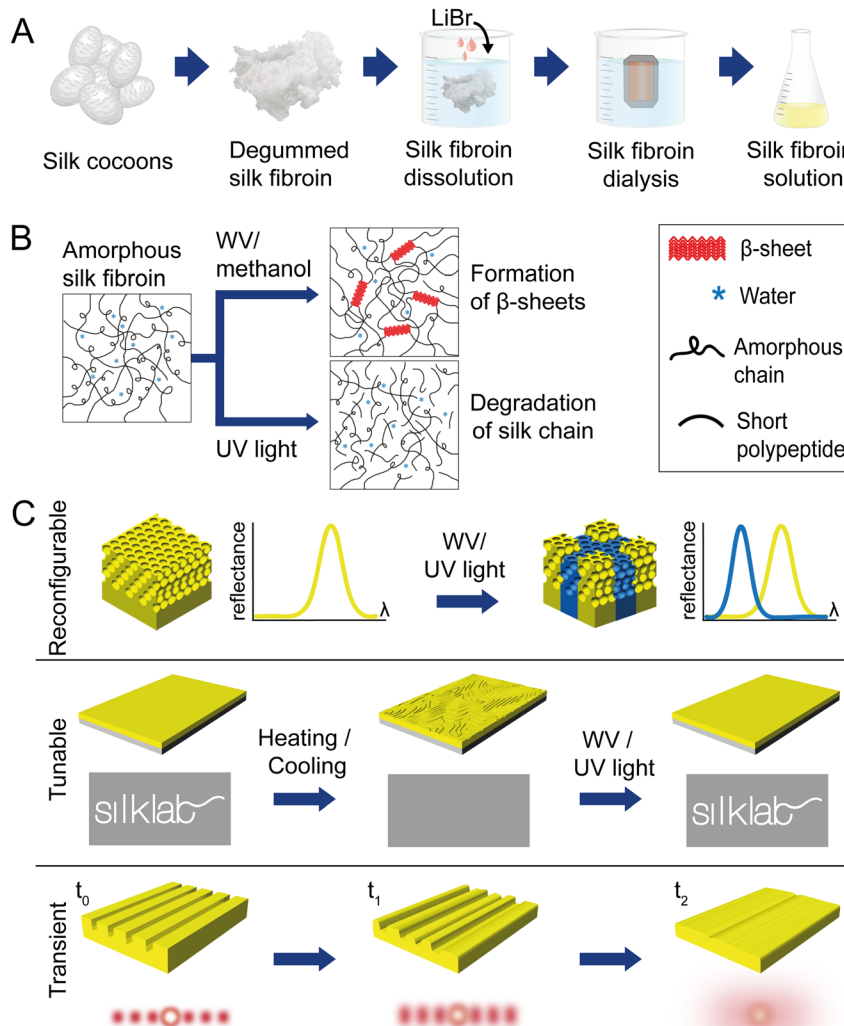


Figure 1: (A) Schematic representation of the silk regeneration process. (B) Schematic representation of amorphous silk fibroin conformational changes induced by water vapor (WV), methanol, and UV light, corresponding, respectively, to the formation of β -sheets and the degradation of the silk chains. Adapted from Ref. [9]. Copyright 2017, WILEY-VCH Verlag GmbH & Co. (C) Representative strategies to obtain reconfigurable, reversibly tunable, and temporally transient silk-based optical structures. Schematic representation of the structure (from top to bottom, silk inverse opal, silk-based wrinkled surface, and silk diffractive optical element) and of the corresponding optical response (from top to bottom, shift of the bandgap position, concealing and revealing of information, and gradual degradation of the diffracted pattern).

abovementioned conformational transitions, allowing for the emergence of physical transient optical devices that can be dissolved in a customized way.

By using the above-described fabrication techniques, silk fibroin solutions can be shaped and programmed to display diverse optical responses. Notably, due to its nanoscale conformability resolution [28], silk can be molded into structures that can display optical functions including lensing and diffractive properties [29, 30], photonic response [9, 13, 20, 31], waveguiding [21], lasing [32], fluorescent response [33], and nonlinear optical behaviors [34–36]. Devices based on these optical functions can be programmed to display an active response by dedicated modifications that ensure silk's transformation abilities. As discussed in detail in the next sections, the main active responses that can be embedded in silk are reconfiguration, reversible tunability, and physical transient behavior (Figure 1C).

3 Active optical devices

3.1 Reconfigurable optics

Silk's polymorphic transitions have been recently harnessed to design silk-based three-dimensional (3D) photonic lattices which can undergo non-reversible conformational changes that affect the construct's optical response. The combination of protein self-assembly with colloidal assembly has been utilized to transform silk aqueous solutions into 3D photonic crystals [9, 23]. The latter is a facile, scalable, and cost-effective manufacturing technique that is widely adopted for the bottom-up fabrication of 3D photonic crystals [37, 38]. The resulting colloidal crystals can be further used as templates for the formation of inverted photonic lattices, which are obtained by template removal through solvent etching. Silk

solutions can readily infiltrate such templates and self-assemble into a freestanding silk film through control over the dynamics of water evaporation. The fabricated silk inverse opals (SIOs) present bright structural colors because of the diffraction of incident light induced by the periodicity of the nanostructures. SIOs can be either amorphous or crystalline depending on the protein's conformation. Since the protein chains in crystalline SIOs are physically crosslinked, this type of photonic lattice is robust and difficult to tune once the structure is fabricated [23]. On the contrary, amorphous SIOs possess a photonic lattice that can be easily modulated under external stimuli, allowing for the fabrication of materials with variable structural color.

Large-scale, highly-ordered, and reconfigurable SIOs have been recently fabricated by using polystyrene sphere multilayers as templates [9]. Instead of using conventional deposition techniques, such templates were prepared by scooping transfer of the floating monolayers at the water/air interface and by stacking them layer-by-layer (Figure 2A). Uniform structural colors were observed as a result of the favorable material characteristics of silk protein, including robust mechanical properties, nanoscale processability, and conformability (Figure 2B). Such

amorphous SIOs are stable at ambient conditions; upon exposure to water vapor or UV light, SIOs' photonic lattice can be controllably compressed along the vertical direction of the film, leading to reconfiguration of the photonic bandgap. This mechanism allows for the generation of structural color over the entire visible spectrum. Multiple multicolor patterns can be easily generated by selectively exposing masked SIOs to water vapor or UV light for different durations (Figure 2C). The underlying mechanism that enables the fabrication of patterned SIOs is the stimuli-induced controllable conformational changes through the molecular rearrangement of silk fibroin.

The above described reconfigurable 3D photonic nanostructures can be further coupled with 2D microscale patterns to fabricate hierarchical photonic structures, where the reconfigurability allows additional functionality by providing extra spectral selectivity. In particular, the combination of silk protein self-assembly, colloidal assembly, and top-down topographical templating has been exploited to integrate 2D diffractive micropatterns with 3D inverse colloidal crystals (Figure 2D–F) [31]. Such hierarchical opals not only embody the convergence of diffusion and diffraction with structural color in a single matrix, but also present a suite of unique optical functions that

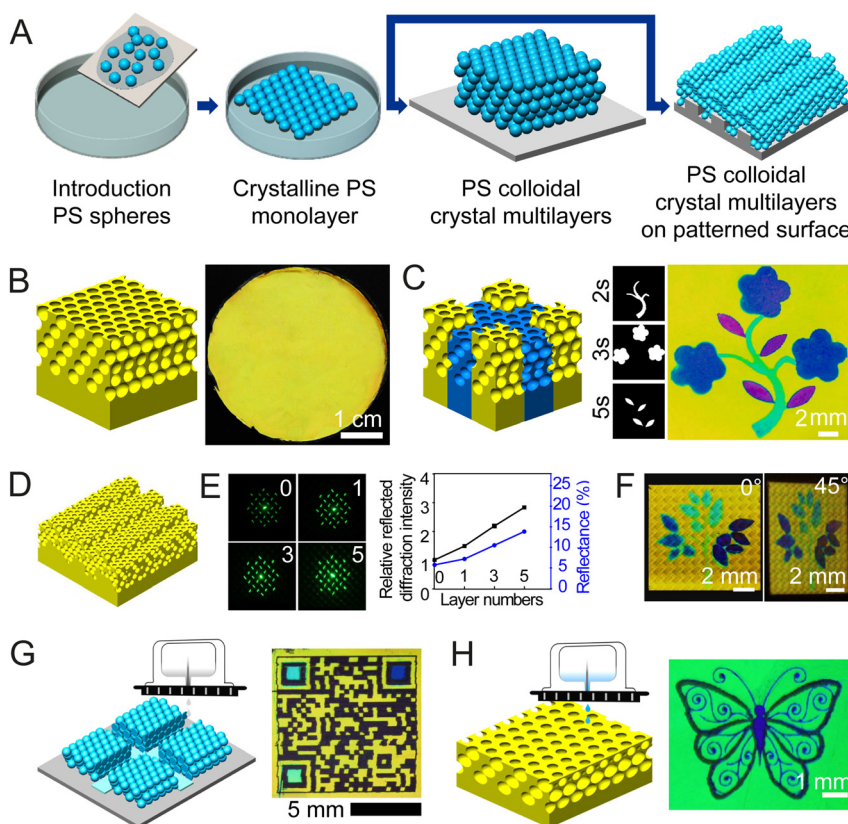


Figure 2: (A) Fabrication schematic of polystyrene sphere multilayer templates on flat and patterned surfaces. (B, C) Schematic (left) and photograph (right) of SIO (B) and patterned SIO (C). (A, B, C) Reproduced from Ref. [9]. Copyright 2017, WILEY-VCH Verlag GmbH & Co. (D) Schematic of hierarchical inverse opal assembled on a diffraction grating; (E) reflected diffraction patterns (left) of hierarchical opals assembled on pattern generators with different layers of inverse colloidal crystals (from 0 to 5) and corresponding relative diffraction and absolute reflection intensity as a function of layers number (right). (F) Photographs of hierarchical opal with a multicolor tree pattern observed at 0° and 45°. (D, E, F) Reproduced from Ref. [31]. Copyright 2018, WILEY-VCH Verlag GmbH & Co. (G) Fabrication schematic (left) of patterned polystyrene multilayer template by depositing ethyl acetate on the structure using inkjet printing and photograph (right) of a multispectral SIO QR code. (H) Fabrication schematic (left) of patterned SIO by depositing MeOH/water mixture on SIO using inkjet printing and photograph (right) of SIO with a butterfly pattern. (G, H) Reproduced from Ref. [20]. Copyright 2019, WILEY-VCH Verlag GmbH & Co.

leverage the interplay of the individual responses. On the one hand, the existence of a 3D nanoscale photonic lattice modulates the diffraction of the 2D optical element by tuning its photonic bandgap; for instance, this can be achieved by controlling the number of layers and the lattice constant of the assembled colloidal crystal or by reconfiguring the photonic lattice by water vapor or UV light treatment. The variation of the reflected (or transmitted) diffraction intensity is consistent with the change of the reflection (or transmission) intensity because of the photonic nanostructure modulation (Figure 2E). On the other hand, the 2D microscale topography affects the overall color appearance of the structures, resulting in uniform structural color over a broad range of viewing angles. Such feature, combined with the reconfigurability of the nanoscale lattice and with the design of multicolor patterns, allows these structures to be used for wide-angle multicolor pattern displays with spatially dependent iridescence (Figure 2F).

The ability to reconfigure photonic lattices provides additional levels of functionality to these engineered photonic crystals, which become structures that not only display multispectral responses but can also be used for information encoding. This has been recently demonstrated by creating multispectral QR codes through the combination of inkjet printing and water vapor treatment (Figure 2G, H) [20]. Inkjet printing was used to modify preassembled photonic crystal lattices to create patterned templates (e.g., a QR code pattern) for silk infiltration and subsequent fabrication of patterned inverse opals. In particular, ethyl acetate was chosen as the ink to selectively remove the photonic lattice in the printed areas, therefore, creating a structure which displayed inverse opal lattices only in the non-printed regions. The resulting SIO QR code was further programmed by exposing specific lattice-bearing regions (colored squares in Figure 2G micrograph) to water vapor for different times, leading to a multispectral QR code with double encryption layers, namely, (i) the scanned message from the QR code, and (ii) a three-digit key defined by the RGB intensity of the reconfigured colors. A reconfigurable SIO itself is an ideal optical platform for pattern writing, which can be achieved by direct integration with inkjet printing and by using a solvent that can trigger the protein's conformational transition (Figure 2H). Different volumetric changes of the silk matrix, and thus distinct differences in the lattice constant and in the reflected colors, can be easily generated by controlling the ink composition or volume. For example, light-blue and dark-blue colors were obtained, respectively, by inkjet printing MeOH/water mixtures with water ratios of 3 and 18% on a 10-layer SIO substrate. This

strategy provides great opportunities for the fabrication of arbitrary, complex, and multispectral photonic patterns by manipulating the protein's initial conformation, the lattice's configuration, and the ink's formulation.

In addition to forming homogeneous inverse opal structures, silk-based reconfigurable photonic crystal superlattices can also be fabricated by stacking layers of 3D nanolattices with different periodicity [39]. Multispectral structural colors can be easily achieved by reconfiguring the lattices of the formed heterostructures by water vapor exposure.

3.2 Reversibly tunable optics

Silk protein materials are also capable of reversibly responding to external stimuli, allowing for the fabrication of dynamic tunable optical devices. Crystalline silk offers an ideal platform for the generation of reversible stimulus-responsiveness, due to its molecular chains being anchored through physical crosslinking. The general strategy for implementing dynamic tunable optical function relies primarily on the reversible volume change of the silk matrix in response to various environmental fluctuations such as humidity, aqueous solvents, mechanical strain, and temperature. Among these, humidity is the most widely utilized stimulus given its ease and speed in inducing swelling of the silk matrix. Silk's high sensitivity to humidity makes silk-based optical devices suitable for sensing applications as demonstrated by the several silk-based optical platforms used to generate dynamic tunable responses to humidity, such as inverse opals [40], thin-film and multilayer interference structures [41, 42], optical fibers [43], and metamaterials [44, 45]. As an example, silk-coated terahertz metamaterials can be programmed to display a dynamic response to humidity changes (Figure 3A), whereby the frequency of the devices is gradually blue-shifted upon humidity increase due to the variation of the dielectric constant of the silk's film induced by the swelling [45]. Another type of reversible responsiveness that relies on the physical swelling of silk matrix is achieved through aqueous solvent infiltration; in this case, the water content in the solvent determines the degree of swelling of the silk constituent within the optical device and thus its optical response. Examples of such tunable devices include metal-insulator-metal resonators using silk protein as the insulator layer [46, 47], and silk plasmonic devices [48]. Mechanically induced tunable optics are based on the continuous and reversible variation of optical structures upon changes in the tensile strain applied to them. In this scenario, silk hydrogels provide an

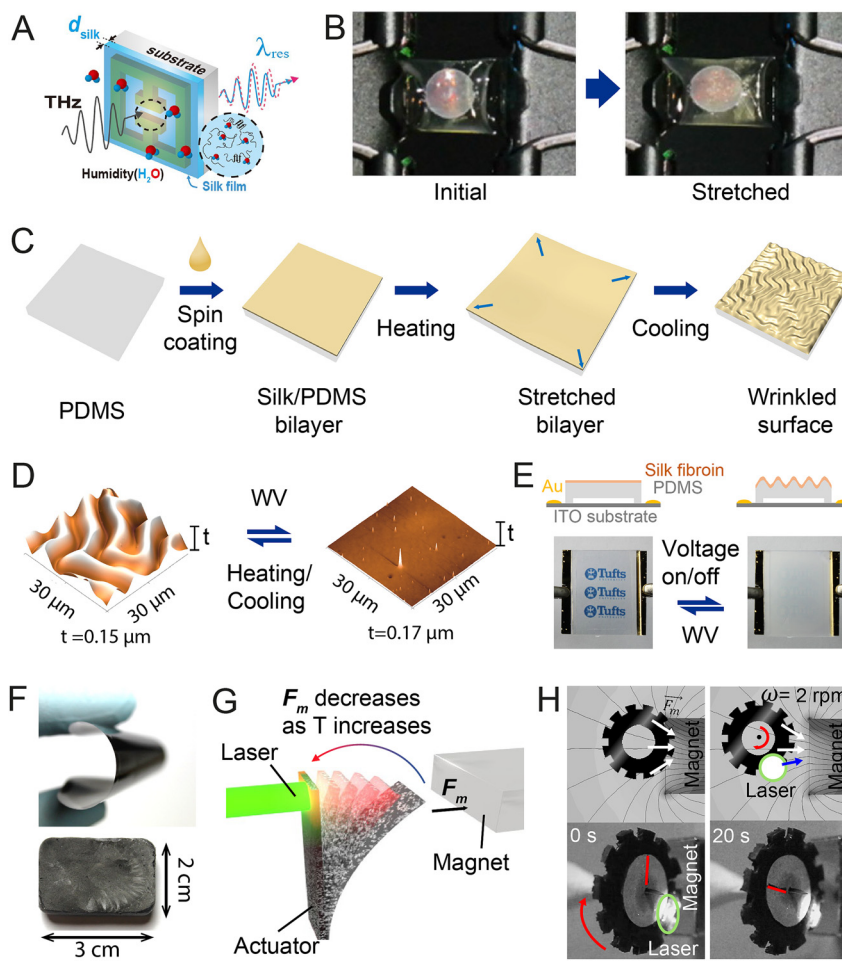


Figure 3: (A) Schematic of humidity sensors based on silk-coated terahertz metamaterials. Reproduced from Ref. [45]. Copyright 2018, OSA publishing, CC BY. (B) Photographs of silk hydrogel inverse opal before (left) and after (right) stretching. Reproduced from Ref. [49]. Copyright 2017, National Academy of Sciences. (C) Fabrication schematic of a silk-based dynamic wrinkle pattern. (D) AFM images showing the reversible transition between wrinkled and wrinkle-free state of the silk-PDMS bilayer film. (E) Schematics (top) and corresponding photographs (bottom) of wrinkle patterns showing the switching between transparent and opaque by respectively exposure to WV and voltage application. (C, D, E) Reproduced from Ref. [51]. Copyright 2019, National Academy of Sciences. (F) Photographs of a magnetic silk film (top) and a silk sponge (bottom) with 50 wt% CrO₂ relative to silk fibroin. (G) Schematic of the actuation mechanism of a cantilever actuator based on heat-induced demagnetization and photothermal effect. (H) Schematics (top) and photographs (bottom) of a Curie engine rotating at 2 rpm under fixed local light illumination and immobile magnet. (F, G, H) Reproduced from Ref. [52]. Copyright 2018, National Academy of Sciences.

ideal material format to transform a mechanical stimulus into an optical response. A typical example is deformable silk hydrogel inverse opals (Figure 3B) [49], in which the elastic deformation of the hydrogel induces a change in the photonic lattice constant of the SIO resulting in reversible changes in the reflected structural color. Further, the large thermal expansion coefficient of silk allows for the development of thermally responsive optical devices. For instance, silk fibroin whispering gallery microresonators showed a significant resonant wavelength shift as a function of temperature, making them suitable for high-precision thermal sensors [50].

Dynamic, tunable optical functions can also be obtained through the combination of two independent stimuli-responsive behaviors. As a demonstration, the polymorphic transition of silk fibroin has been combined with its thermal responsiveness to develop reversible and dynamic wrinkling micropatterns [51]. These wrinkling systems consist of a bilayer structure composed of a stiff silk thin layer and a soft PDMS substrate. The mechanical

mismatch between these two materials induces the formation of a wrinkled surface after application of thermal stimuli (Figure 3C). This wrinkle pattern accumulates compressive stress after its formation and can be tuned or erased through molecular rearrangement of silk with either water vapor, methanol vapor, or exposure to UV light (Figure 3D); these treatments cause the continuous disturbance of the localized stress field and the subsequent release of the compressive stress within the bilayer system. The wrinkles' dynamics depend on the initial conformation of the silk film, showing that wrinkle tuning is governed by the interplay between silk protein chains and external stimuli. The switchable wrinkle morphology (Figure 3E), together with the versatility of silk protein, enables applications such as wearable optics, information coding, and thermal management.

Furthermore, reversible stimuli-responsiveness can be achieved by doping silk solutions with optically active components, adding functionality to mechanically robust and biocompatible platforms. One demonstration of this

strategy is the fabrication of magnetic composites by incorporating chromium dioxide (CrO_2) in multiple silk formats such as films and sponges (Figure 3F) [52]. The low Curie temperature of CrO_2 along with its high photothermal conversion efficiency allows for the generation of a tunable magnetic response as a function of light, leading to light-controlled and dynamically tunable motions activated by fixed light source and magnetic field (Figure 3G, H). Devices fabricated from these composites show multiple complex locomotions, such as oscillation, gripping, and heliotactic movements, along with continuous rotation (Figure 3H). In addition to solution mixing, optical functionality can also be embedded in silk-based materials by chemical modification of the silk protein by taking advantage of its abundant surface chemistry. For instance, the incorporation of azobenzene moieties into silk structures creates a photo-responsive biomaterial (Azosilk) [53–55], whose optical absorption can be tuned by leveraging the reversible photo-switching between the *trans* and *cis* geometric isomers of azobenzene molecules. Optically switchable diffractive gratings have been developed by integrating an Azosilk grating with an elastomeric substrate, where the diffraction properties can be reversibly modulated by switching the light on and off [55].

3.3 Physically transient optics

Physically transient devices are programmed to either display an on/off signal or a modulation of their response as a function of time. Silk has been recently demonstrated to be a compelling material for the fabrication of both bio-electronic [56–58] and optically transient devices [15, 33, 59, 60] mostly due the ability to modulate its degradation. By properly tuning the cross-linking degree of the silk construct, its functional lifetime can be precisely programmed into the material so that it retains its structural integrity, and therefore, its form and optical functions, for a precise amount of time (from minutes to years) behaving as an intrinsically temporally transient device [24, 25]. The correlation between the silk structural degradation and the device's optical response variation enables the fabrication of devices which can display an intrinsic, self-reporting, and continuous monitoring system. Silk-based transient devices find applications in drug delivery, resorbable implants and information security.

Silk's high cytocompatibility [61, 62], and ability to stabilize labile compounds [63] have been exploited to use silk as a platform for drug-delivery devices. Therefore, silk-based transient optical devices can be particularly useful for the fabrication of comprehensive biomedical devices

which simultaneously feature drug stabilization, controlled drug release and optical feedback (indirect drug release monitoring). The optical signature of these devices depends on their structural integrity and, if present, on the dopant type and loading [30]. Typically, silk fibroin is first mixed with therapeutics [19], and then molded into an optical element, such as microprism arrays [3], diffraction optical elements (DOEs) [15, 64], or fluorescent fibers [33], and finally annealed through water/methanol treatments to tune its degradation time. The progressive proteolytic cleaving of silk promotes the drug release while affecting the device's form and, therefore, its optical response (Figure 4A). In particular, the amount of drug released can be correlated to changes in reflectivity for prism arrays [3] and to variations of the photoluminescent intensity and spectral position for fluorescent silk fibers [33]. For monochromatic DOEs, the signal-to-noise ratio (SNR) of the diffracted signal is used, instead, for the optical feedback: the simultaneous dissolution of the device and the release of the drug induce physical and chemical deterioration of the DOE (Figure 4B), leading to a progressive disappearance of the diffracted pattern and, therefore, to a decrease of the SNR [15, 18] (Figure 4C). The SNR variation can be correlated to the amount of drug released and, therefore, used as a self-monitoring system. Multiple drug release can also be monitored at the same time by embedding each one in a different component of multichromatic DOEs [64]. Depending on the silk conformation state, these devices can be programmed not only to lose their optical imprint within a specific timeframe but also to fully dissolve. This kind of transient devices provides monitoring of the therapeutic release while eliminating the need for retrieval of the drug-support system after completion of their functional lifetimes.

Another simple yet elegant application of transient silk DOEs is for information security, in which the variation of the refractive index contrast is used to create transient patterns. Silk DOEs can display three operation modes: information concealment, information reappearance, and information destruction (Figure 4D–F). The information is first encoded by designing the structure of the DOE, it can then be revealed by illuminating the DOE with the specific wavelength it has been optimized for, and it can be further destroyed by degrading the microstructure of the DOE through silk dissolution. Information concealment is achieved by using a combination of silk and another material with similar refractive index and by exploiting the variation of the refractive index contrast. For instance, a DOE pattern fabricated on glass ($n_{\text{glass}} \sim 1.52$) can be clearly visualized when exposed to air and illuminated with a laser beam; its message can then be temporarily hidden by

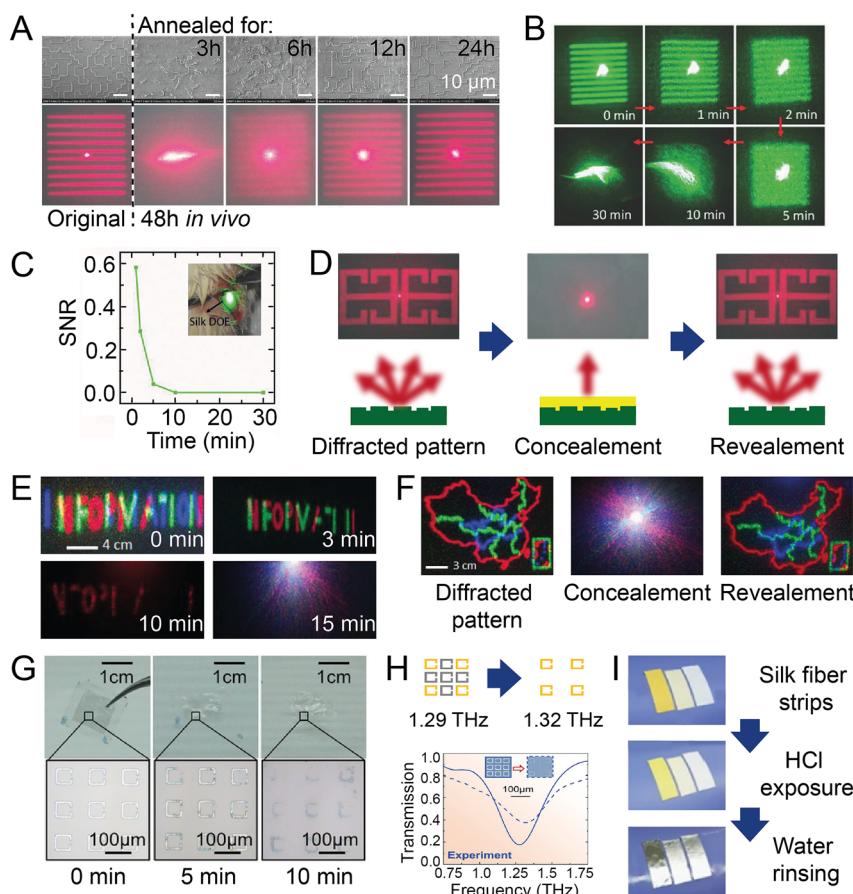


Figure 4: (A) Effect of the annealing time (3, 6, 12, and 24 h) on silk DOEs structure degradation (top row, SEM images) and on the corresponding optical response (bottom row, diffracted pattern) as quantified after 48 h *in vivo*. (B) Reflected diffraction patterns of a drug-doped silk DOE at different times showing the progressive degradation of the diffracted signal. (C) Variation of the surface-to-noise ratio (SNR) of the DOE as a function of time. Inset: picture of the DOE implanted on the skin of a rat on an infection site. (D) Diffracted pattern (top) and schematics of the structure (bottom) demonstrating information concealment and reappearance obtained by combining a glass DOE (green) with a silk coating (yellow). (A, B, C, D) Adapted from Ref. [15]. Copyright 2017, WILEY-VCH Verlag GmbH & Co. (E) Silk multi-colored DOE with multiple crystallinity degrees: the blue DOE starts degrading after 3 min, the red DOE after 10 min and the blue DOE after 15 min leading to gradual destruction of the information. (F) Glass multi-colored DOE showing information concealment and reveal due to, respectively, the application and the removal of a silk coating. (E, F) Adapted from Ref. [64]. Copyright 2018, Shanghai Institute of Microsystem and Information Technology (SIMIT), Chinese Academy of Sciences

(CAS). Published by WILEY-VCH Verlag GmbH & Co. (G) Multi-metal metamaterials on silk substrates immersed in deionized water for 0, 5, and 10 min. (H) Schematic of multi-metal metamaterials on silk substrates showing the variation of the split ring resonator unit (top) and of the corresponding resonance (bottom) as a function of metals solubility. (G, H) Reproduced from Ref. [65]. Copyright 2020, WILEY-VCH Verlag GmbH & Co. (I) Doped fluorescent silk nanofiber strips after exposure to HCl vapors and after water rinsing. Adapted from Ref. [33]. Copyright 2017, The Authors.

covering it with a silk coating ($n_{\text{silk}} \sim 1.54$) that creates optical continuity by strongly decreasing the refractive index contrast and, therefore, it nullifies the DOE effect (Figure 4D); the pattern can, then, be further revealed by removal of the silk layer, which can, again, be intrinsically programmed by tuning the silk crystallinity [15].

Multichromatic silk-based DOEs enable multilevel encryption by containing multiple DOEs, each one optimized to work at a specific wavelength (Figure 4E, F) [64]. Notably, the degradation rate and sequence can be independently tuned for each monochromatic DOE, therefore enabling individual functional lifetimes for each diffracting pattern. This vanishing DOE system can store both temporally and chromatic dependent information. Multichromatic DOEs can also be used for quantitatively monitoring chemical reactions by embedding solid reagents in silk DOEs and by immersing them in a liquid reagent to trigger the reaction; the monitoring of the variation of the

SNR and of the optical density of the DOEs as the reaction progresses allows to obtain quantitative information on the formed products, provided prior calibration [64]. In addition, transient silk-based distributed feedback (DFB) lasers can be fabricated by repeated application and dissolution of a dye-doped silk solution on diffraction gratings [60].

Based on the same operation principle of controlled silk degradation, metamaterial devices able to work as transient, implantable and drug-delivery systems have been fabricated by patterning split ring resonators made of electrically conductive, biocompatible, and biodegradable metals on flexible silk substrates [65]. Both the metamaterial and the silk substrate can be programmed to independently affect the time-dependent resonance frequency response, respectively, by controlling the initial conformation of the silk matrix, as previously discussed (Figure 4G), and by using metals with different dissolution rates (Figure 4H). The ability to selectively remove

structural components of the actual resonating structures (for instance achieved by using metals with different solubilities) allows for further complexity in the overall metamaterial response and in the structure's degradation path. Notably, small changes in the structure of the metamaterial induce significant variations in the inductance and capacitance, therefore, inducing a shift in the resonant response and making these devices suitable for high precision monitoring. Though these devices are currently operating in the terahertz regime, they could be fabricated to display an optical response in the visible range useful, for instance, for *in vivo* sensing and for information encryption.

The low cost of silk-based transient optical devices makes them ideal for the fabrication of, for instance, disposable acid vapor sensors. Fluorescent electrospun silk fibers doped with sodium fluorescein have been, indeed, reported as high precision, disposable, low cost and conformable sensors for highly toxic acid vapors, such as HCl (Figure 4I) [33]. Fluorescent silk fiber patches can detect HCl in a broad range of concentrations (5–300 ppm) inducing a deterioration in the photoluminescent signal and a variation of its spectral position upon exposure to the vapor. Due to silk's biocompatibility and tunability, it is possible to apply these sensors directly on the skin and to program them to vanish upon water rinsing without creating environmental hazards [33].

4 Conclusion and outlook

Regenerated silk fibroin has become a compelling material platform for the fabrication of active optical systems that are able to sense and transform diverse external stimuli into specific optical signals. This technological use of such an ancient material has been enabled by the protein's intrinsic properties, which include controllable conformational transitions, reversible physical swelling and shrinking, and programmable biodegradation in response to external physical and chemical perturbations. The past decade has witnessed a continuous growth in the development of silk-based stimuli-responsive optical devices, including reconfigurable photonic crystals, reversibly tunable optical structures, and physically transient devices. These stimuli-responsive optical systems, together with the biological traits of silk, enable the fabrication of wearable, disposable, and implantable devices with multiple functionalities, and thus drive application opportunities toward, but not limited to, bio- and environmental sensing, smart displays, information encoding, and drug delivery systems with self-monitoring capabilities.

While silk has shown great potential for the development of active optics, many scientific and technological challenges still need to be overcome for silk-based devices to fulfill their full potential. For instance, in spite of the opportunities enabled by the conformational transitions of silk, some critical questions remain unanswered: (i) how to fabricate "structurally patterned" silk matrices with high resolution over large areas; (ii) how to spatially and precisely control the protein's conformation in thick structures (e.g., thicker than a few tens of micrometers). In addition, for silk-based bio-/environmental sensors, their sensitivity, response rate, and selectivity must be further improved to meet the specific requirements of practical sensing applications. Furthermore, it is still challenging to achieve precise control over the degradation process of silk materials given the difficulty in precisely controlling the degree of crystallinity, film thickness, and the molecular weight of the protein. Other compelling critical concerns include the inherent batch-to-batch variability of silk solutions, the scale-up production and processing, the devices' integration, long-term durability, conformance, and cost; these have not yet been adequately addressed and thus significantly impede the use of silk-based active optical devices for commercial applications. These challenges can be solved by a comprehensive understanding of the "structure–property–process–function" relationships of silk protein.

The use of a versatile biopolymer material format (silk protein) as a stimuli-responsive platform for active optical devices provides a sustainable alternative to traditional inorganic materials, semiconductors, and non-biodegradable synthetic polymers. Although a lot of progress has been made in silk-based dynamic optical devices, several directions should be payed attention to and be explored in the future. First, the current studies have mainly focused on the fabrication of active optical systems with well-defined single stimuli-responsive behaviors, and thus single output signals. Devices accommodating multiple dynamic behaviors provide emerging opportunities toward intelligent optics. The combinations of protein self-assembly, top-down transformation technologies, and silk's ease of functionalization are promising avenues for the development of these devices. Another interesting direction is the creation of optically functionalized and stimuli-responsive silk platforms, such as optomechanical, photoluminescent, and chromogenic materials, through either chemical modification of the silk protein or genetic engineering to insert specific optical functional domains into the molecular sequences of silk. In addition, it is worthwhile to exploit silk-based active optical materials with different formats, scales, and geometries. Promising

strategies for this research direction involve the integration of protein self-assembly with other manufacturing techniques including 3D/4D printing, microfluidic technology, and origami/kirigami. Furthermore, silk provides an excellent stimuli-responsive material platform to interface optics with the biological world due to its comprehensive mechanical, biological, and optical properties. Current focuses on this territory are primarily on silk-based transient optical devices by leveraging the degradation process of silk matrix. In the future, efforts need to be also devoted to developing non-transient, active silk bio-optical devices for chronic epidermal and *in vivo* applications. The key to this purpose is to extend the lifetime of silk matrix at ambient conditions for skin-mounted devices and in wet media for silk implants through, for example, accurately controlling the structural organization from the nano- to the macroscale. Last but not least, nonlinear optical properties observed in natural silk fibers can be an interesting output signals for the future development of silk-based dynamic optics for sensing applications. Finally, interdisciplinary collaborations constitute a further step toward the goal of devising the next-generation of silk-based sustainable, active, and intelligent optical devices that can subtly, adaptively, and multiply respond to environmental changes in a wide variety of application fields.

Acknowledgments: The authors would like to acknowledge support from the Office of Naval Research (grant N00014-19-1-2399).

Author contribution: All the authors have accepted responsibility for the entire content of this submitted manuscript and approved submission.

Research funding: The authors would like to acknowledge support from the Office of Naval Research (grant N00014-19-1-2399).

Conflict of interest statement: The authors declare no conflicts of interest regarding this article.

References

- [1] K. A. Arpin, A. Mihi, H. T. Johnson, et al., "Multidimensional architectures for functional optical devices," *Adv. Mater.*, vol. 22, pp. 1084–1101, 2010.
- [2] T. Asakura, Y. Sato, and A. Aoki, "Stretching-induced conformational transition of the crystalline and noncrystalline domains of 13C-labeled bombyx mori silk fibroin monitored by solid state NMR," *Macromolecules*, vol. 48, pp. 5761–5769, 2015.
- [3] H. Tao, J. M. Kainerstorfer, S. M. Siebert, et al., "Implantable, multifunctional, bioresorbable optics," *Proc. Natl. Acad. Sci. U. S. A.*, vol. 109, pp. 19584–19589, 2012.
- [4] H. J. Jin and D. L. Kaplan, "Mechanism of silk processing in insects and spiders," *Nature*, vol. 424, pp. 1057–1061, 2003.
- [5] R. F. P. Pereira, M. M. Silva, and V. De Zea Bermudez, "Bombyx mori silk fibers: an outstanding family of materials," *Macromol. Mater. Eng.*, vol. 300, pp. 1171–1198, 2015.
- [6] F. Chen, D. Porter, and F. Vollrath, "Structure and physical properties of silkworm cocoons," *J. R. Soc. Interface*, vol. 9, pp. 2299–2308, 2012.
- [7] C. Dicko, J. M. Kenney, and F. Vollrath, "β-Silks: enhancing and controlling aggregation," *Adv. Protein Chem.*, vol. 73, pp. 17–53, 2006.
- [8] D. N. Rockwood, R. C. Preda, T. Yücel, X. Wang, M. L. Lovett, and D. L. Kaplan, "Materials fabrication from *Bombyx mori* silk fibroin," *Nat. Protoc.*, vol. 6, pp. 1612–1631, 2011.
- [9] Y. Wang, D. Aurelio, W. Li, et al., "Modulation of multiscale 3D lattices through conformational control: painting silk inverse opals with water and light," *Adv. Mater.*, vol. 29, pp. 1–9, 2017.
- [10] B. Marelli, N. Patel, T. Duggan, et al., "Programming function into mechanical forms by directed assembly of silk bulk materials," *Proc. Natl. Acad. Sci. U. S. A.*, vol. 114, pp. 451–456, 2017.
- [11] K. Yazawa, K. Ishida, H. Masunaga, T. Hikima, and K. Numata, "Influence of water content on the β-sheet formation, thermal stability, water removal, and mechanical properties of silk materials," *Biomacromolecules*, vol. 17, pp. 1057–1066, 2016.
- [12] Z. Zhou, S. Zhang, Y. Cao, B. Marelli, X. Xia, and T. H. Tao, "Engineering the future of silk materials through advanced manufacturing," *Adv. Mater.*, vol. 30, p. 1706983, 2018.
- [13] S. Kim, B. Marelli, M. A. Brenckle, et al., "All-water-based electron-beam lithography using silk as a resist," *Nat. Nanotechnol.*, vol. 9, pp. 306–310, 2014.
- [14] N. Qin, S. Zhang, J. Jiang, et al., "Nanoscale probing of electron-regulated structural transitions in silk proteins by near-field IR imaging and nano-spectroscopy," *Nat. Commun.*, vol. 7, 2016. <https://doi.org/10.1038/ncomms13079>.
- [15] Z. Zhou, Z. Shi, X. Cai, et al., "The use of functionalized silk fibroin films as a platform for optical diffraction-based sensing applications," *Adv. Mater.*, vol. 29, p. 1605471, 2017.
- [16] R. K. Pal, N. E. Kurland, C. Wang, S. C. Kundu, and V. K. Yadavalli, "Biopatterning of silk proteins for soft micro-optics," *ACS Appl. Mater. Interfaces*, vol. 7, pp. 8809–8816, 2015.
- [17] M. A. Brenckle, H. Tao, S. Kim, M. Paquette, D. L. Kaplan, and F. G. Omenetto, "Protein-protein nanoimprinting of silk fibroin films," *Adv. Mater.*, vol. 25, pp. 2409–2414, 2013.
- [18] J. P. Mondia, J. J. Amsden, D. Lin, L. D. Negro, D. L. Kaplan, and F. G. Omenetto, "Rapid nanoimprinting of doped silk films for enhanced fluorescent emission," *Adv. Mater.*, vol. 22, pp. 4596–4599, 2010.
- [19] H. Tao, B. Marelli, M. Yang, et al., "Inkjet printing of regenerated silk fibroin: from printable forms to printable functions," *Adv. Mater.*, vol. 27, pp. 4273–4279, 2015.
- [20] W. Li, Y. Wang, M. Li, L. P. Garbarini, and F. G. Omenetto, "Inkjet printing of patterned, multispectral, and biocompatible photonic crystals," *Adv. Mater.*, vol. 31, p. 1901036, 2019.
- [21] S. T. Parker, P. Domachuk, J. Amsden, et al., "Biocompatible silk printed optical waveguides," *Adv. Mater.*, vol. 21, pp. 2411–2415, 2009.
- [22] D. Lin, H. Tao, J. Trevino, et al., "Direct transfer of subwavelength plasmonic nanostructures on bioactive silk films," *Adv. Mater.*, vol. 24, pp. 6088–6093, 2012.

[23] S. Kim, A. N. Mitropoulos, J. D. Spitzberg, H. Tao, D. L. Kaplan, and F. G. Omenetto, "Silk inverse opals," *Nat. Photonics*, vol. 6, pp. 818–823, 2012.

[24] X. Hu, K. Shmelev, L. Sun, et al., "Regulation of silk material structure by temperature-controlled water vapor annealing," *Biomacromolecules*, vol. 12, pp. 1686–1696, 2011.

[25] Q. Lu, X. Hu, X. Wang, et al., "Water-insoluble silk films with silk I structure," *Acta Biomater.*, vol. 6, pp. 1380–1387, 2010.

[26] A. Sagnella, A. Pistone, S. Bonetti, et al., "Effect of different fabrication methods on the chemo-physical properties of silk fibroin films and on their interaction with neural cells," *RSC Adv.*, vol. 6, pp. 9304–9314, 2016.

[27] J. Shao, J. Zheng, J. Liu, and C. M. Carr, "Fourier transform Raman and Fourier transform infrared spectroscopy studies of silk fibroin," *J. Appl. Polym. Sci.*, vol. 96, pp. 1999–2004, 2005.

[28] H. Perry, A. Gopinath, D. L. Kaplan, L. D. Negro, and F. G. Omenetto, "Nano- and micropatterning of optically transparent, mechanically robust, biocompatible silk fibroin films," *Adv. Mater.*, vol. 20, pp. 3070–3072, 2008.

[29] B. D. Lawrence, M. Cronin-Golomb, I. Georgakoudi, D. L. Kaplan, and F. G. Omenetto, "Bioactive silk protein biomaterial systems for optical devices," *Biomacromolecules*, vol. 9, pp. 1214–1220, 2008.

[30] P. Domachuk, H. Perry, J. J. Amsden, D. L. Kaplan, and F. G. Omenetto, "Bioactive "self-sensing" optical systems," *Appl. Phys. Lett.*, vol. 95, p. 253702, 2009.

[31] Y. Wang, W. Li, M. Li, et al., "Biomaterial-based "structured opals" with programmable combination of diffractive optical elements and photonic bandgap effects," *Adv. Mater.*, vol. 31, 2019. <https://doi.org/10.1002/adma.201970030>.

[32] S. Caixeiro, M. Gaio, B. Marelli, F. G. Omenetto, and R. Sapienza, "Silk-based biocompatible random lasing," *Adv. Opt. Mater.*, vol. 4, pp. 998–1003, 2016.

[33] K. Min, S. Kim, C. G. Kim, and S. Kim, "Colored and fluorescent nanofibrous silk as a physically transient chemosensor and vitamin deliverer," *Sci. Rep.*, vol. 7, 2017. <https://doi.org/10.1038/s41598-017-05842-8>.

[34] W. L. Rice, S. Firdous, S. Gupta, et al., "Non-invasive characterization of structure and morphology of silk fibroin biomaterials using non-linear microscopy," *Biomaterials*, vol. 29, pp. 2015–2024, 2008.

[35] S. Kujala, A. Mannila, L. Karvonen, K. Kieu, and Z. Sun, "Natural silk as a photonics component: a study on its light guiding and nonlinear optical properties," *Sci. Rep.*, vol. 6, 2016. <https://doi.org/10.1038/srep22358>.

[36] Y. Zhao, K. T. T. Hien, G. Mizutani, and H. N. Rutt, "Second-order nonlinear optical microscopy of spider silk," *Appl. Phys. B Lasers Opt.*, vol. 123, p. 188, 2017.

[37] N. Vogel, M. Retsch, C. A. Fustin, A. Del Campo, and U. Jonas, "Advances in colloidal assembly: the design of structure and hierarchy in two and three dimensions," *Chem. Rev.*, vol. 115, pp. 6265–6311, 2015.

[38] K. R. Phillips, G. T. England, S. Sunny, et al., "A colloidoscope of colloid-based porous materials and their uses," *Chem. Soc. Rev.*, vol. 45, pp. 281–322, 2016.

[39] Y. Wang, M. Li, E. Colusso, W. Li, and F. G. Omenetto, "Designing the iridescences of biopolymers by assembly of photonic crystal superlattices," *Adv. Opt. Mater.*, vol. 6, pp. 1–7, 2018.

[40] Y. Y. Diao, X. Y. Liu, G. W. Toh, L. Shi, and J. Zi, "Multiple structural coloring of silk-fibroin photonic crystals and humidity-responsive color sensing," *Adv. Funct. Mater.*, vol. 23, pp. 5373–5380, 2013.

[41] Q. Li, N. Qi, Y. Peng, et al., "Sub-micron silk fibroin film with high humidity sensibility through color changing," *RSC Adv.*, vol. 7, no. 29, pp. 17889–17897, 2017.

[42] E. Colusso, G. Perotto, Y. Wang, M. Sturaro, F. Omenetto, and A. Martucci, "Bioinspired stimuli-responsive multilayer film made of silk-titanate nanocomposites," *J. Mater. Chem. C*, vol. 5, pp. 3924–3931, 2017.

[43] K. Hey Tow, D. M. Chow, F. Vollrath, I. Dicaire, T. Gheysens, and L. Thevenaz, "Exploring the use of native spider silk as an optical fiber for chemical sensing," *J. Light. Technol.*, vol. 36, pp. 1138–1144, 2018.

[44] H. Tao, J. J. Amsden, A. C. Strikwerda, et al., "Metamaterial silk composites at terahertz frequencies," *Adv. Mater.*, vol. 22, pp. 3527–3531, 2010.

[45] H. S. Kim, S. H. Cha, B. Roy, S. Kim, and Y. H. Ahn, "Humidity sensing using THz metamaterial with silk protein fibroin," *Opt. Express*, vol. 26, p. 33575, 2018.

[46] H. Kwon and S. Kim, "Chemically tunable, biocompatible, and cost-effective metal-insulator-metal resonators using silk protein and ultrathin silver films," *ACS Photonics*, vol. 2, pp. 1675–1680, 2015.

[47] S. Arif, M. Umar, and S. Kim, "Interacting metal-insulator-metal resonator by nanoporous silver and silk protein nanomembranes and its water-sensing application," *ACS Omega*, vol. 4, pp. 9010–9016, 2019.

[48] M. Lee, H. Jeon, and S. Kim, "A highly tunable and fully biocompatible silk nanoplasmmonic optical sensor," *Nano Lett.*, vol. 15, p. 49, 2015.

[49] K. Min, S. Kim, and S. Kim, "Deformable and conformal silk hydrogel inverse opal," *Proc. Natl. Acad. Sci. U. S. A.*, vol. 114, pp. 6185–6190, 2017.

[50] L. Xu, X. Jiang, G. Zhao, et al., "High-Q silk fibroin whispering gallery microresonator," *Opt. Express*, vol. 24, p. 20825, 2016.

[51] Y. Wang, B. J. Kim, B. Peng, et al., "Controlling silk fibroin conformation for dynamic, responsive, multifunctional, micropatterned surfaces," *Proc. Natl. Acad. Sci. U. S. A.*, vol. 116, pp. 21361–21368, 2019.

[52] M. Li, Y. Wang, A. Chen, et al., "Flexible magnetic composites for light-controlled actuation and interfaces," *Proc. Natl. Acad. Sci. U. S. A.*, vol. 115, pp. 8119–8124, 2018.

[53] M. Cronin-Golomb, A. R. Murphy, J. P. Mondia, D. L. Kaplan, and F. G. Omenetto, "Optically induced birefringence and holography in silk," *J. Polym. Sci. B*, vol. 50, pp. 257–262, 2011.

[54] M. J. Landry, M. B. Applegate, O. S. Bushuyev, et al., "Photo-induced structural modification of silk gels containing azobenzene side groups," *Soft Matter*, vol. 13, pp. 2903–2906, 2017.

[55] G. Palermo, L. Barberi, G. Perotto, et al., "Conformal silk-azobenzene composite for optically switchable diffractive structures," *ACS Appl. Mater. Interfaces*, vol. 9, pp. 30951–30957, 2017.

[56] L. Sun, Z. Zhou, N. Qin, and T. H. Tao, "Transient multi-mode silk memory devices," in *Proceedings of the IEEE International Conference on Micro Electro Mechanical Systems (MEMS)*, vol. 2019-Janua, Institute of Electrical and Electronics Engineers Inc., 2019, pp. 519–521.

[57] M. A. Brenckle, H. Cheng, S. Hwang, et al., "Modulated degradation of transient electronic devices through multilayer

silk fibroin pockets," *ACS Appl. Mater. Interfaces*, vol. 7, no. 36, pp. 19870–19875, 2015.

[58] S. W. Hwang, H. Tao, D. H. Kim, et al., "A physically transient form of silicon electronics," *Science*, vol. 337, pp. 1640–1644, 2012.

[59] S. Toffanin, S. Kim, S. Cavallini, et al., "Low-threshold blue lasing from silk fibroin thin films," *Appl. Phys. Lett.*, vol. 101, p. 91110, 2012.

[60] H. Jung, K. Min, H. Jeon, and S. Kim, "Physically transient distributed feedback laser using optically activated silk bio-ink," *Adv. Opt. Mater.*, vol. 4, pp. 1738–1743, 2016.

[61] C. Vepari and D. L. Kaplan, "Silk as a biomaterial," *Prog. Polym. Sci.*, vol. 32, pp. 991–1007, 2007.

[62] A. R. Murphy and D. L. Kaplan, "Biomedical applications of chemically-modified silk fibroin," *J. Mater. Chem.*, vol. 19, pp. 6443–6450, 2009.

[63] J. A. Kluge, A. B. Li, B. T. Kahn, D. S. Michaud, F. G. Omenetto, and D. L. Kaplan, "Silk-based blood stabilization for diagnostics," *Proc. Natl. Acad. Sci. U. S. A.*, vol. 113, pp. 5892–5897, 2016.

[64] X. Cai, Z. Zhou, and T. H. Tao, "Programmable vanishing multifunctional optics," *Adv. Sci.*, vol. 6, p. 1801746, 2019.

[65] L. Sun, Z. Zhou, J. Zhong, et al., "Implantable, degradable, therapeutic terahertz metamaterial devices," *Small*, vol. 16, p. 2000294, 2020.